

## Mechanisms of jamming in the Nagel-Schreckenberg model for traffic flow

Henrik M. Bette,<sup>1,2,\*</sup> Lars Habel,<sup>2,†</sup> Thorsten Emig,<sup>1,3,4,‡</sup> and Michael Schreckenberg<sup>2,§</sup>

<sup>1</sup>Multi-Scale Materials Science for Energy and Environment, (MSE)<sup>2</sup>, UMI 3466, Joint CNRS-MIT Laboratory, Massachusetts Institute of Technology, 77 Massachusetts Avenue, Cambridge, Massachusetts 02139, USA

<sup>2</sup>Universität Duisburg-Essen, Physik von Transport und Verkehr, 47058 Duisburg, Germany

<sup>3</sup>Massachusetts Institute of Technology, Department of Physics, Cambridge, Massachusetts 02139, USA

<sup>4</sup>Laboratoire de Physique Théorique et Modèles Statistiques, CNRS UMR 8626, Bât. 100, Université Paris-Sud, 91405 Orsay cedex, France

(Received 4 August 2016; published 12 January 2017)

We study the Nagel-Schreckenberg cellular automata model for traffic flow by both simulations and analytical techniques. To better understand the nature of the jamming transition, we analyze the fraction of stopped cars  $P(v = 0)$  as a function of the mean car density. We present a simple argument that yields an estimate for the free density where jamming occurs, and show satisfying agreement with simulation results. We demonstrate that the fraction of jammed cars  $P(v \in \{0, 1\})$  can be decomposed into the three factors (jamming rate, jam lifetime, and jam size) for which we derive, from random walk arguments, exponents that control their scaling close to the critical density.

DOI: [10.1103/PhysRevE.95.012311](https://doi.org/10.1103/PhysRevE.95.012311)

### I. INTRODUCTION

The modeling of traffic is a common field of application for cellular automata (CA) models. Based on empirical studies in the context of the three-phase traffic theory by Kerner [1], complex CA models have been developed and studied, e.g., in Refs. [2–4]. These are conceptually based on the model described by Nagel and Schreckenberg [5], which displays only two different regimes for different densities, free flow and congestion. Despite its simplicity, no exact results have yet been obtained for the NaSch-CA except in some limiting cases [6,7].

In the NaSch-CA, a vehicle  $i$  at time  $t$  is defined by its position  $x_i$  and velocity  $v_i$ .  $d_i = x_{i+1} - x_i - 1$  denotes the gap between vehicles  $i$  and  $i + 1$ . The movement of vehicle  $i$  from time step  $t$  to  $t + 1$  is then defined by the well-known rules:

- (1) Acceleration:

$$v_i^{(1)} = \min(v_i(t) + 1, v_{\max}),$$

- (2) Deceleration:

$$v_i^{(2)} = \min(d_i(t), v_i^{(1)}),$$

- (3) Randomized braking (dawdling):

$$v_i(t + 1) = \max(v_i^{(2)} - 1, 0), \text{ with probability } p,$$

- (4) Movement:

$$x_i(t + 1) = x_i(t) + v_i(t + 1).$$

Even though being a nonequilibrium system, many observations made in the NaSch-CA have been compared to equilibrium systems. Among them is the comparison to the phase transition between liquid and vapor [8], where one does not have a clear transition between all-liquid state and all-vapor

state at a certain temperature. Instead, a continuous change in the amount of molecules in the liquid phase and the vapor phase occurs. This is very interesting as this behavior is similar to the one in the NaSch-CA. Instead of all vehicles suddenly becoming jammed at a certain density, more and more jamming occurs during an increase of the overall density of cars [9].

There have been approaches put forward to consider the lifetimes of these jams in order to establish criteria for a phase transition. Nagel [10] observed these numerically, while Gerwinski [11] tried an analytic approach to calculate the critical density from the stability of jams. In Ref. [11] it was argued that stopped vehicles can be found at any density, as long as there are more vehicles than the maximum velocity  $v_{\max}$ .

Recently Ref. [12] took a closer look at the velocity statistics in the NaSch-CA and presented a possibly noncontinuous transition in the probability to find a stopped vehicle. However, improved simulations performed for the present work show that the impression of a noncontinuity turns out to be a finite-size effect, and the aforementioned argument in Ref. [11] remains valid. Finite-size effects have also been investigated recently by Balouchi [13]. The continuous transition is, however, very interesting, especially considering the probability distribution functions presented in Ref. [12] as they show an almost zero probability for any velocities except for  $v_{\max}$  or  $v_{\max} - 1$  in the free-flow regime. Therefore, we argue that stopped vehicles are at least a good indicator for existing jams, although not being a genuine order parameter for a finite number  $v_{\max}$  of velocity levels. Reference [14] describes a related approach to see  $p$  as an external field that renders the sharp transition continuous. Appendix B shows the difference between their order parameter and the indicator presented in Sec. II.

This work distinguishes the mechanisms that lead to the sudden increase in the existence of these jammed cars. In Sec. II we provide an approach to estimate the crossover density inspired by the comparison to the liquid-vapor transition. In Sec. III we analyze the mechanisms that control the formation of jams by decomposing the number of jammed vehicles into three different factors: the jamming rate, the

\*henrik.bette@uni-due.de

†lars.habel@uni-due.de

‡emig@mit.edu

§michael.schreckenberg@uni-due.de

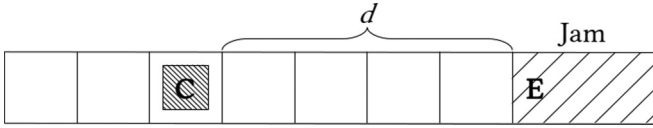


FIG. 1. A car **C** that will end up behind the end of the jam **E**, if it is not dawdling, as the cells in between are empty.

lifetime of jams, and their total number of cars. From a random walk argument, we obtain the exponents that describe the scaling of these factors with density. We find good agreement with our simulation results.

## II. FREE DENSITY WITH JAMS

During the liquid-vapor transition, an equilibrium exists between the probabilities for molecules to evaporate from liquid into vapor and to condense from vapor into liquid, which is established due to the pressure in the vapor phase. Analogously, a jam in the NaSch-CA can be compared to the liquid having a constant density  $\rho_j = 1$ , whereas in the free flow regime a varying free density  $\rho_f$  can be observed, which corresponds to the pressure of the vapor. It is evident that a higher free density will lead to an increased probability  $P_{in}$  for vehicles to end up in a jam and a decreased probability  $P_{out}$  to leave a jam, just as higher vapor pressure leads to more molecules condensing into liquid and less evaporation.

Solving the equation

$$P_{in}(\rho_f) = P_{out}(\rho_f) \quad (1)$$

for  $0 \leq \rho_f < 1$  then yields the minimal free density, at which stable jams can be observed. Here we assume that  $\rho_f$  is constant outside of a jam, which, of course, is an approximation as local densities can fluctuate [9]. Also, the aforementioned velocity statistics presented in Ref. [12] indicate that deceleration and acceleration around jams can be neglected for total densities inside the free-flow regime of the model.

To approximate  $P_{in}(\rho_f)$ , we consider up to  $d = v_{max}$  cells upstream of a jam; see Fig. 1. Here a jam is defined as a chain of standing vehicles with a free cell at the upstream end. For simplicity, we assume an equal distribution of cars in the upstream cells given by  $\rho_f$ . In this mean-field approach [15], the probability to find a car at distance  $d$  with all cells empty between **C** and **E** is

$$\tilde{P} = \rho_f(1 - \rho_f)^{d-1}. \quad (2)$$

Note that the cell directly behind the jam is empty by definition.

Due to the randomization parameter  $p$ ,  $0 \leq p \leq 1$ , it is possible that cars with  $d < v_{max}$  will overbrake and leave a cell empty behind **E** when stopping. It is reasonable to consider these cars jammed as well, because of their immediate interaction with the jam. In the case of  $d = v_{max}$ , however, a dawdling car, i.e., accounted for by rule 3, cannot immediately interact with the jam, whereas a nondawdling car ends up in the jam. For  $d = v_{max}$ , Eq. (2) has to be multiplied by  $q = 1 - p$  and all cases  $d > v_{max}$  do not contribute. Summing over all distances, the probability that there is a car behind the jam

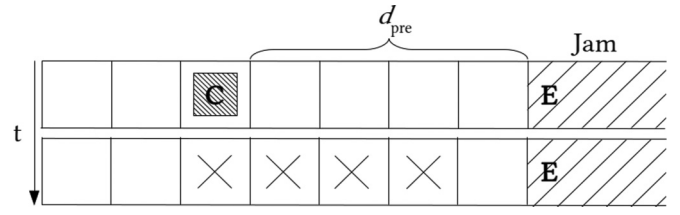


FIG. 2. A car **C** will block cells for the next time step as no car can overtake or arrive at distance  $d \leq d_{pre}$ .

which will end up in it is

$$\tilde{P}_{in}(v_{max}) = \sum_{d=1}^{v_{max}} Q(d) \rho_f (1 - \rho_f)^{d-1}, \quad (3)$$

where

$$Q(d) = \begin{cases} q & \text{if } d = v_{max} \\ 1 & \text{otherwise.} \end{cases} \quad (4)$$

First results have shown that this simple approximation should be improved by incorporating a restriction due to single-lane traffic: Without overtaking, a car can only be at any position  $d$  if no car entered the jam from a distance  $d_{pre} \geq d$  in the preceding time step; see Fig. 2. This can be corrected by

$$P_{corr}(d) = \sum_{s=d}^{v_{max}} Q(s) \rho_f (1 - \rho_f)^{s-1} = \tilde{P}_{in}(v_{max}) - \tilde{P}_{in}(d), \quad (5)$$

which is the probability that a car was at  $d_{pre} \geq d$ . Note that this correction does not consider two time steps directly.

Taking this into account, the corrected probability  $P_{in}$  to find a car behind the jam which will end up in it can be written as

$$P_{in}(v_{max}) = \sum_{d=1}^{v_{max}} Q(d) \rho_f (1 - \rho_f)^{d-1} [1 - P_{corr}(d)]. \quad (6)$$

Obviously, the stopping car **C** would actually move the end of the jam **E** one cell backwards, which would complicate the whole estimation. To maintain comparability to the liquid-vapor transition, we have omitted this fact and consider the jam as a particle reservoir that will immediately fill the cell of a leaving car. Therefore, head and tail of the jam are assumed to be immovable on small time scales.

The probability  $P_{out}$  depends on  $q$  for the starting car at the front of the jam. Because of the one-directional movement, the area immediately in front of the jam is governed by the cars leaving the jam, and therefore  $P_{out}$  does not depend on  $\rho_f$  in contrast to the liquid-vapor transition. Using Eq. (6), we also have to consider a dependency on the preceding step, when defining  $P_{out}$  in order to be consistent. This is shown in Fig. 3, where the so-defined immovable jam front prevents a second car from starting in the next time step.  $P_{out}$  is then given by

$$P_{out} = \frac{q}{2}. \quad (7)$$

By solving Eq. (1) for  $\rho_f$ , we can determine the free density for which jams will be “stable”. In this approach, the free flow density is assumed to stay constant for  $\rho > \rho_f$  as more and more cars are jammed. For densities lower than  $\rho_f$ , one

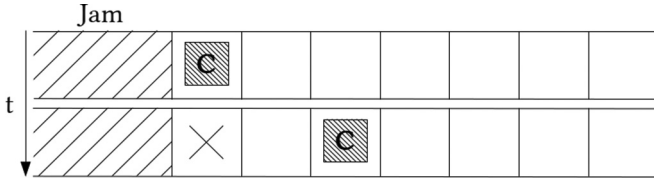


FIG. 3. Only one car **C** can leave the jam in succeeding time steps if the jam front is considered immovable. In the depicted situation, **C** moves without dawdling.

should have almost no stopped vehicles, although this number will never be exactly zero due to fluctuations [11]. Once  $\rho_f$  is reached, one should see an increase in the number of stopped vehicles.

We performed simulations of the NaSch-CA with  $p = 0.5$  and different  $v_{\max}$ , starting with periodic boundary conditions and equally spaced vehicles with  $v = 0$ . The system parameters have been chosen so that no finite size effects occur [13]; see Table I for values of the system length  $L$ , the relaxation time  $T_{\text{relax}}$ , and the measurement time  $T_{\text{meas}}$ .

Figure 4 shows the measured probabilities  $P(v = 0)$  to find a standing vehicle and the numerically calculated  $\rho_f$  from Eq. (1). For the simple approximation we made, the onset of a significant  $P(v = 0)$  and  $\rho_f$  show convincing agreement, in particular for higher  $v_{\max}$ . Clearly, for small  $v_{\max}$  a significant number of cars is already stopped below  $\rho_f$ , because an interaction of  $v_{\max}$  cars is sufficient to stop a car with a certain probability [11]. This is more likely for small  $v_{\max}$ , wherefore the transition becomes steeper for higher  $v_{\max}$ . There the number of velocity states a car can assume increases, and a zero velocity state becomes less probable. This means that when density fluctuations become more important in the proximity of  $\rho_f$ , they have a stronger effect on the number of stopped cars for smaller  $v_{\max}$ . The increase of  $P(v = 0)$  beyond  $\rho_f$  in Fig. 4 does not result from these fluctuations. An explanation for this will be given in Sec. III.

Figure 4 also indicates that  $\rho_f \rightarrow 0$  for  $v_{\max} \rightarrow \infty$ . In Appendix A, we show analytically that  $\rho_f = q/(2v_{\max})$  in that limit.

If all cars inside a jam were stopped and all cars (numbered by  $i \in \{1, \dots, N\}$ ) outside moved with velocities  $v_i \geq v_{\max} - 1$ , the maximum of the flow, classically defined as

$$J = \frac{1}{L} \sum_{i=1}^N v_i, \quad (8)$$

TABLE I. System parameters and the calculated  $\rho_f$ .

$v_{\max}$ [cells/time steps]	$L$ [cells]	$T_{\text{relax}}, T_{\text{meas}}$ [time steps]	$\rho_f$ [1/cells]
3	$10^4$	$\geq 10^6$	0.1206
4	$2 \times 10^4$	$\geq 10^6$	0.0892
5	$2 \times 10^4$	$\geq 10^6$	0.0708
7	$10^5$	$\geq 10^6$	0.0502
10	$2 \times 10^5$	$\geq 10^6$	0.0350

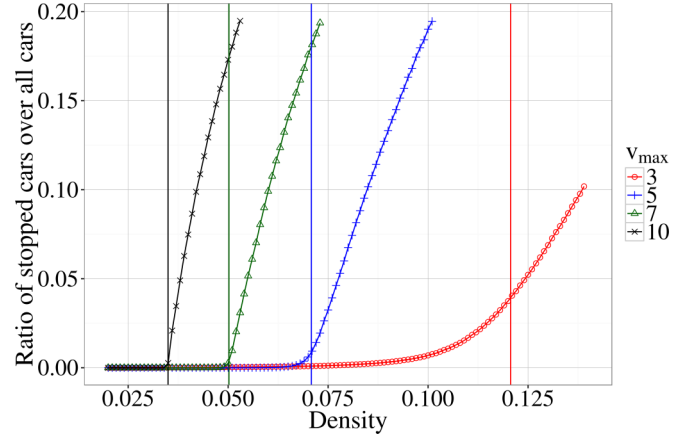


FIG. 4. Probability  $P(v = 0)$  to find a standing car for different  $v_{\max}$  as a function of mean car density. The horizontal lines show the calculated values for  $\rho_f$  obtained from Eq. (1).

should appear at  $\rho_f$ . Due to a more complex velocity distribution [12] with nonzero probabilities for velocities between 1 and  $v_{\max} - 2$ , the free density  $\rho_f$  is not the same as the critical density  $\rho_c$  defined as the point where the maximum flow is reached (see Fig. 5). Such a transitional behavior has been suggested in Ref. [9] for  $0 < p < 1$ .

### III. MECHANISMS OF JAM FORMATION

In order to establish a better understanding of the mechanisms that lead to the sudden rise of stopped vehicles shown in Fig. 4, it is useful to take a closer look at the statistics of jamming at low densities, which allows for distinguishing the different mechanisms. Due to computational limits, we have excluded the case  $v_{\max} = 10$  in the following.

The logarithmic plot of the number of jammed vehicles in Fig. 6 shows a nonvanishing amount even for very low densities. Obviously, the equations developed in Sec. II do not capture this behavior. Considering the different slopes in

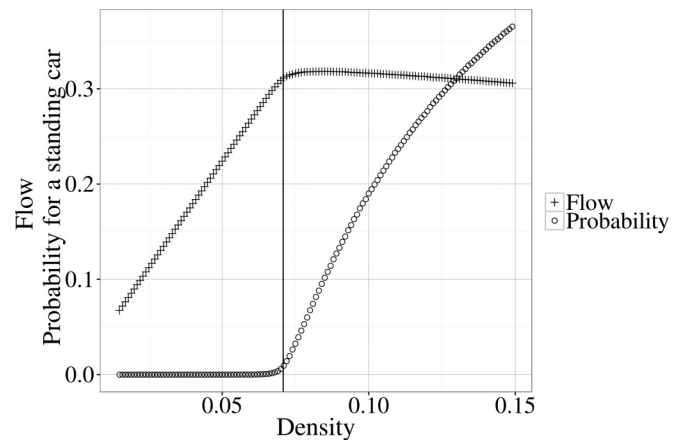


FIG. 5. Normalized number of stopped cars  $P(v = 0)$  compared with the global flow  $J$  for simulations with  $v_{\max} = 5$ . The vertical line shows the calculated  $\rho_f$ . The amount of stopped cars begins to rise before the maximum flow is reached. This is mainly due to cars in jams not having a vanishing average velocity.

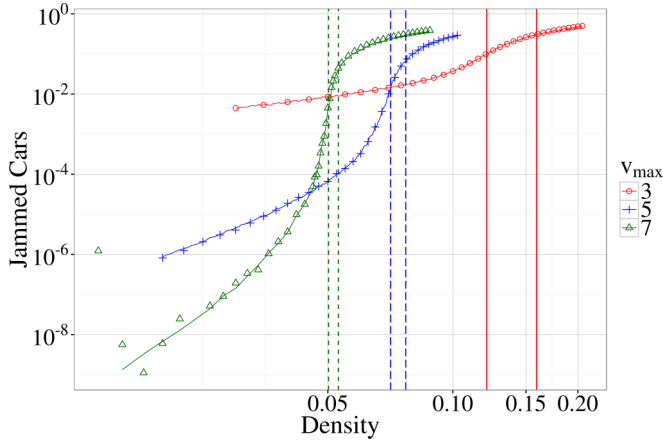


FIG. 6. Comparison of the directly measured ratio of jammed cars (points) and the product of the individually measured three factors (lines): jamming rate, jam lifetime, and cars in a jam. Two vertical lines represent the calculated free density and the critical density obtained from the fundamental diagram.

Fig. 6 it seems reasonable to expect at least two different mechanisms: One that leads to a power-law rise of the number of jammed vehicles even at very low densities and another one that only sets in slightly below the density of maximum flow and results in the observed stronger increase just below the critical density.

When looking at the system at any fixed time step, we can distinguish three factors that determine the number of jammed cars. New jams will be formed out of free-flow-fluctuations with a certain “jamming rate”, previously formed jams will still be present, if they appeared no longer ago than their lifetime  $\tau_{\text{jam}}$ , and each of these jams contributes a certain amount to the total number of jammed cars. To have a quantitative comparison between the directly measured number of jammed cars  $N_{\text{jam}}$  and the one calculated from the factors, we define a car to be jammed if  $v \leq 1$  instead of  $v = 0$  from now on.  $N_{\text{jam}}$  should then be the product of these three factors and that this is indeed correct can be seen in Fig. 6, which shows  $N_{\text{jam}}$  and the three individual factors. To measure the mentioned jam properties in the simulations, we used the labeling algorithm suggested in Ref. [10] with an adjusted definition for a jammed car. Here every jam gets a label  $lbl$ , a starting time  $t_{\text{start}}(lbl)$  and an ending time  $t_{\text{end}}(lbl)$ . At each time step  $t$ , all nonjammed cars are assigned the label 0 with  $t_{\text{start}}(0) = t + 1$ , whereas every jammed car is assigned the label of the oldest jam that influenced it by comparing the starting times. This can either be a jam, from which it has not accelerated yet, an older jam, of which the car in front was part of, or a new one. Last, the ending time of all currently existing labels is set to  $t$ , meaning that the jam lifetime is determined by a vanishing label.

While the considerations in Sec. II cannot capture the jamming rate, they should predict the approximate point at which the lifetime of traffic jams will undergo a significant change. However, it is not obvious if this will have any effect on the number of cars in a jam. We postulate that the jamming rate will be important in the power-law rise for very low densities, while the lifetime will be responsible for the steep rise near the critical density.

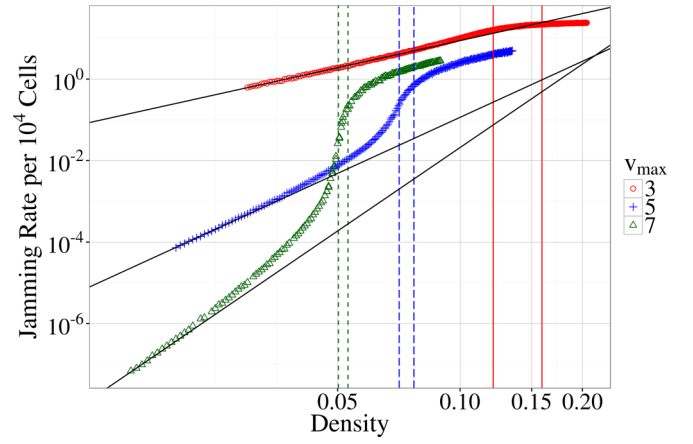


FIG. 7. The rate at which traffic jams form for different maximum velocities. Two vertical lines represent the calculated free density and the critical density; black lines represent fitting in the low-density region. Here a power-law behavior  $\propto \rho^{v_{\text{max}}-1}$  is visible as expected and described by Ref. [11]. The rise near the free density for  $v_{\text{max}} > 3$  is closely related to the cutoff in jam lifetimes at that point and results from the measuring algorithm.

Our conjecture is strongly supported by the results shown in Figs. 7 and 8. From Fig. 8 we can see that  $N_{\text{jam}}$  undergoes almost the same change as the lifetime  $\tau_{\text{jam}}$  of these jams. Therefore, we can reason that these two observables are closely related and can be expected to be linked by a simple physical process. We conclude that the rate at which jams form is responsible for a nonvanishing amount of jammed vehicles at very low densities. In Ref. [11] it has been suggested that the number of jammed cars for low densities scales as  $\rho^{v_{\text{max}}-1}$ . Extrapolating fits for the slope of the jamming rate to a density of zero confirms exactly this behavior; see Fig. 7. The sudden increase in the number of jammed vehicles  $N_{\text{jam}}$  below the density of maximum flow is caused by the stabilization of

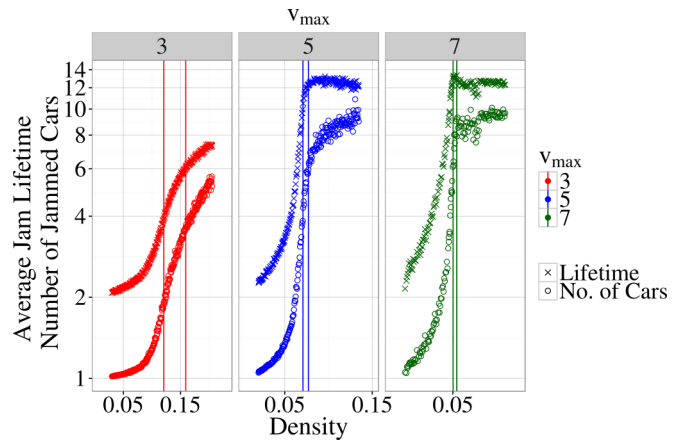


FIG. 8. The average lifetime of traffic jams and the average number of cars therein for different maximum velocities. The two vertical lines represent the calculated free density and the critical density. Near the free density a steep rise in the lifetime of jams is observable. For maximum velocities greater than three a sharp cutoff in the lifetime is visible. This is due to the definition of “jammed cars” used for the measurement.



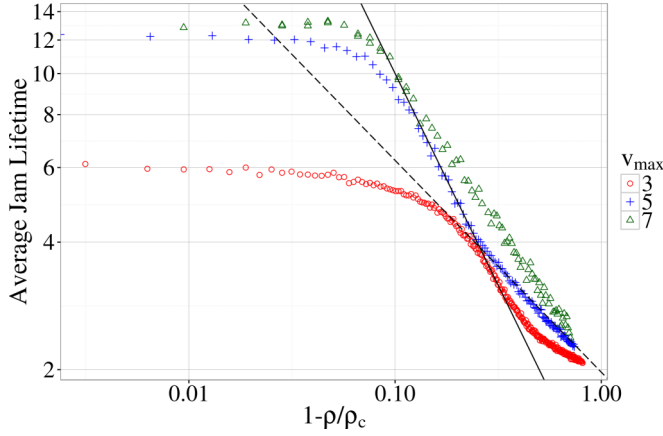


FIG. 9. The average lifetime of a traffic jam plotted over a rescaled density  $\bar{\rho} = 1 - (\rho/\rho_c)$ . The rise near the critical density can be seen to behave proportional to  $(\rho_c - \rho)^{-1}$  (solid lines). An earlier rise for low-density seems to scale with  $(\rho_c - \rho)^{-1/2}$  (dashed lines).

these jams, i.e., longer lifetimes. As our equal probability argument considered above to estimate the free density is basically a stability criterion, it is satisfying that the values for the free density lie in the region of the steep rise in lifetime.

Comparing the curves in Fig. 8, it is obvious that longer living jams include proportionally more cars. This effect together with the strict definition of “jammed cars” used to obtain the data, leads to the here observed saturation in the jam lifetimes. As the jams get bigger, it becomes more probable that a car will accelerate to  $v > 1$  for a very short time without actually leaving the jam. This means the car will be considered nonjammed by our labeling algorithm. It therefore tends to recognize big jams as a cluster of small jams. Seemingly big jams fragment into small jams of an average lifetime around 13 time steps and including slightly less than 10 cars. When using the original definition for “jammed cars” proposed in Ref. [10], no strong deviation from the power-law behavior can be found in the jamming rate.

While our simulation results for the jamming rate at low densities can be compared to existing theory that predicts a power law (see Fig. 7), there is lack of arguments explaining the observed scaling of the average number of jammed cars  $N_{\text{jam}}$  and the lifetime of jams  $\tau_{\text{jam}}$ . Just below the critical density but before saturation effects occur, we observe the approximative scaling

$$\tau_{\text{jam}} \propto (\rho_c - \rho)^{-1}, \quad (9a)$$

$$N_{\text{jam}} \propto (\rho_c - \rho)^{-1}; \quad (9b)$$

see solid lines in Figs. 9 and 10. The range over which this scaling is observed is cutoff by saturation effects that set in well before  $\rho_c$  is reached. However, the data for the largest  $v_{\text{max}} = 7$  suggest that this is the proper scaling close to  $\rho_c$  in the large  $v_{\text{max}}$  limit.

In the following, we shall use simple random walk arguments to derive these scaling laws in the limit of large  $v_{\text{max}}$ .

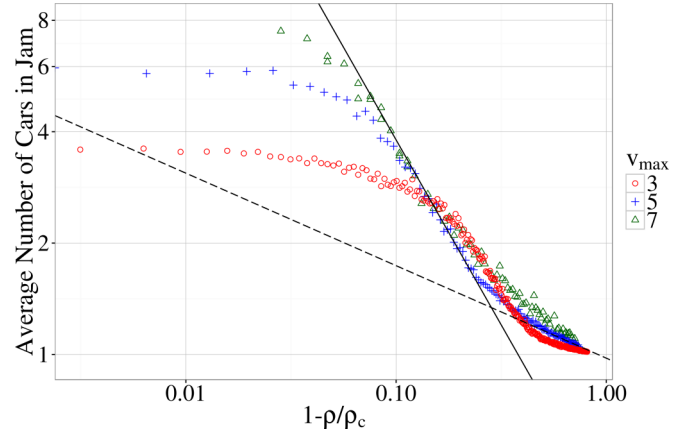


FIG. 10. The average number of cars in a traffic jam plotted over a rescaled density  $\bar{\rho} = 1 - (\rho/\rho_c)$ . The rise near the critical density can be seen to behave proportionally to  $(\rho_c - \rho)^{-1}$  (solid line). An earlier rise for low-density seems to scale with  $(\rho_c - \rho)^{-1/4}$  (dashed line).

Related arguments have been given for the lifetime of a jam of fixed initial length [16]. The number of cars  $N_{\text{jam}}(t)$  within a given jam at  $t$  time steps can be considered as a biased random walk process. The effective probabilities for  $N_{\text{jam}}$  to increase (decrease) are

$$P = P_{\text{in}}(1 - P_{\text{out}})/(P_{\text{in}} + P_{\text{out}} - 2P_{\text{in}}P_{\text{out}}), \quad (10a)$$

$$Q = 1 - P = P_{\text{out}}(1 - P_{\text{in}})/(P_{\text{in}} + P_{\text{out}} - 2P_{\text{in}}P_{\text{out}}), \quad (10b)$$

where  $P_{\text{in}}$  and  $P_{\text{out}}$  are the probabilities for flow in or out of a jam; see Sec. II, which in the low-density (or high  $v_{\text{max}}$ ) limit are approximated by  $P_{\text{in}} = \rho v_{\text{max}}$  (see Appendix A) and  $P_{\text{out}} = (1 - \rho)/2$ . In this random walk picture, the lifetime of a jam is described by the probability distribution

$$P_{\text{ret}}(t) = \binom{t}{t/2} (PQ)^{t/2} / [2P(t-1)] \quad (11)$$

that the walker returns to zero, i.e.,  $N_{\text{jam}} = 0$ , for the first time after  $t$  steps (which must be even). This distribution yields the mean lifetime  $\tau_{\text{jam}} = 2(1 - P)/(1 - 2P)$ . Since  $1 - 2P \propto \rho_c - \rho$ , the result of Eq. (9a) follows. To obtain the scaling of  $N_{\text{jam}}$  we consider the mean absorption time  $\tau_{\text{jam}} \propto N_{\text{jam}}/(1 - 2P)$  when the walker has reached  $N_{\text{jam}}$ . Since also  $N_{\text{jam}} \propto \tau_{\text{jam}}^{1/2}$ , we find  $N_{\text{jam}} \propto 1/(1 - 2P)$  and hence the result of Eq. (9b). We expect the density range over which these scaling forms can be observed to grow with  $v_{\text{max}}$ . Hence, simulations at substantially larger values for  $v_{\text{max}}$  are desirable to probe these predictions.

In the limit of vanishing densities, to leading order, we observe from our simulation results a different behavior that approaches the power laws:

$$\tau_{\text{jam}} \propto (\rho_c - \rho)^{-1/2}, \quad (12a)$$

$$N_{\text{jam}} \propto (\rho_c - \rho)^{-1/4}; \quad (12b)$$

see dashed lines in Figs. 9 and 10. It is interesting that even at low densities these quantities seem to scale with the distance from the critical density  $\rho_c - \rho$ . While the two power laws are related by a random walk relation  $N_{\text{jam}} \propto \tau_{\text{jam}}^{1/2}$ , the above arguments do not apply due to the very small size of the jams, typically one to two cars. Since a jammed car is defined in our simulations as a car with  $v \leq 1$ , it needs at least two time steps to leave the jammed state with  $v = 0$ . Since the probability for increasing the velocity of an individual car by one unit in a time step is  $\propto \tau_{\text{jam}}^{-1}$  one expects  $\tau_{\text{jam}}^{-2} \propto P_{\text{out}} - P_{\text{in}} \propto \rho_c - \rho$ , which reproduces the observed scaling.

#### IV. CONCLUSION

In the present work, we established better understanding of the mechanisms of jamming in the NaSch-CA.

Therefore, an approach to determine the density of the jamming transition based on a stability criterion was presented. The calculated free densities show good agreement with simulations. Afterwards, we decomposed the ratio of jammed cars into different mechanisms, which allowed us to conclude that, while jams already form at very low densities, increasing jam lifetimes lead to the transition. This is underlined by the initial ansatz being based on jam stabilization.

Furthermore, it was shown that the suggested power-law behavior for low densities [11] originates from the formation of new jams. Using random walk arguments, we derived explanations for the behavior of the jam lifetime and the number of cars in a jam slightly below the critical density.

#### ACKNOWLEDGMENTS

H.M.B. acknowledges support from the UMI 3466 during his visit at MIT. L.H. has been supported by Deutsche Forschungsgemeinschaft (DFG) within the Collaborative Research Center SFB 876, project B4. The authors thank M. Kardar for useful discussions and comments.

#### APPENDIX A: EXACT SOLUTION OF EQ. (1)

FOR  $v_{\text{max}} \rightarrow \infty$

Let  $\bar{\rho}_f = 1 - \rho_f$ . First, Eq. (5) can be split up into two parts to allow for inserting of Eq. (4),

$$P_{\text{corr}}(d) = \frac{\rho_f}{\bar{\rho}_f} \sum_{s=d}^{v_{\text{max}}-1} \bar{\rho}_f^s + q\rho_f \bar{\rho}_f^{v_{\text{max}}-1},$$

and, using the geometric series relation (with  $0 \leq \bar{\rho}_f < 1$ ), it results in

$$\begin{aligned} P_{\text{corr}}(d) &= \frac{\rho_f}{\bar{\rho}_f} \frac{\bar{\rho}_f^d - \bar{\rho}_f^{v_{\text{max}}}}{1 - \bar{\rho}_f} + q\rho_f \bar{\rho}_f^{v_{\text{max}}-1} \\ &= \bar{\rho}_f^{d-1} + \bar{\rho}_f^{v_{\text{max}}-1} (q\rho_f - 1). \end{aligned} \quad (\text{A1})$$

For  $v_{\text{max}} \geq 2$ , the sum in Eq. (6) can also be split up to allow for inserting Eqs. (A1) and (4),

$$\begin{aligned} P_{\text{in}}(v_{\text{max}}) &= \sum_{d=1}^{v_{\text{max}}-1} \rho_f \bar{\rho}_f^{d-1} [1 - \bar{\rho}_f^{d-1} - (q\rho_f - 1) \bar{\rho}_f^{v_{\text{max}}-1}] \\ &\quad + \underbrace{q\rho_f \bar{\rho}_f^{v_{\text{max}}-1} [1 - \bar{\rho}_f^{v_{\text{max}}-1} - (q\rho_f - 1) \bar{\rho}_f^{v_{\text{max}}-1}]}_R, \end{aligned} \quad (\text{A2})$$

where the abbreviation  $R$  was introduced.

Further transformations and the use of the geometric series relation yield

$$\begin{aligned} P_{\text{in}}(v_{\text{max}}) &= \rho_f \frac{1 - \bar{\rho}_f^{v_{\text{max}}-1}}{1 - \bar{\rho}_f} [1 - (q\rho_f - 1) \bar{\rho}_f^{v_{\text{max}}-1}] \\ &\quad - \rho_f \frac{1 - \bar{\rho}_f^{2v_{\text{max}}-2}}{1 - \bar{\rho}_f^2} + R. \end{aligned} \quad (\text{A3})$$

In the case of  $v_{\text{max}} \rightarrow \infty$ , Eq. (A3) can be simplified to

$$\lim_{v_{\text{max}} \rightarrow \infty} P_{\text{in}}(v_{\text{max}}) = \frac{\rho_f}{1 - \bar{\rho}_f} - \frac{\rho_f}{1 - \bar{\rho}_f^2}. \quad (\text{A4})$$

Inserting Eq. (A4) into Eq. (1) yields the polynomial function

$$\rho_f^2(2 - q) + \rho_f(2q - 2) = 0. \quad (\text{A5})$$

Equation (A5) has two real solutions  $\rho_f = 0$  and  $\rho_f = \frac{2q-2}{2-q}$ . Because of  $0 \leq q \leq 1$ , the latter requires densities  $\rho_f \leq 0$ . Therefore,  $\rho_f = 0$  is the only meaningful solution.

The solution  $\rho_f = 0$  allows for conducting a Taylor expansion of Eq. (6) at  $\rho_f = 0$ , which yields  $P_{\text{in}} = 0 + \rho_f v_{\text{max}} + O(\rho_f^2)$ . For high  $v_{\text{max}}$  this leads to

$$\rho_f = \frac{q}{2v_{\text{max}}}. \quad (\text{A6})$$

#### APPENDIX B: DIFFERENCE BETWEEN PHASE PARAMETERS

This work has studied an indicator

$$m = P(v = 0) = 1 - P(v > 0) \quad (\text{B1})$$

for the transition from free flow to congestion.

In Ref. [14] a parameter  $M$  defined as

$$M = 1 - \frac{j}{v_{\text{max}} \rho} \quad (\text{B2})$$

was used for this purpose. There  $j$  is the locally measured traffic flow. With  $\bar{v}$  as the average velocity we can then use  $j = \rho \bar{v}$  and get

$$M = 1 - \frac{\bar{v}}{v_{\text{max}}} = 1 - \frac{\sum_{u=1}^{v_{\text{max}}} u P(v = u)}{v_{\text{max}}}. \quad (\text{B3})$$

Therefore  $M \neq m$  if  $v_{\text{max}} > 1$ .

- [1] B. S. Kerner, *Introduction to Modern Traffic Flow Theory and Control: The Long Road to Three-Phase Traffic Theory* (Springer, Berlin, Heidelberg, 2009).
- [2] W. Knospe, L. Santen, A. Schadschneider, and M. Schreckenberg, *J. Phys. A* **33**, L477 (2000).
- [3] B. S. Kerner, S. L. Klenov, and D. E. Wolf, *J. Phys. A* **35**, 9971 (2002).
- [4] D. Jost and K. Nagel, *Transport Res. Rec.* **1852**, 152 (2003).
- [5] K. Nagel and M. Schreckenberg, *J. Phys. I (France)* **2**, 2221 (1992).
- [6] K. Nagel and H. J. Herrmann, *Physica A* **199**, 254 (1993).
- [7] M. Sasvári and J. Kertész, *Phys. Rev. E* **56**, 4104 (1997).
- [8] A. Schadschneider, D. Chowdhury, and K. Nishinari, *Stochastic Transport in Complex Systems: From Molecules to Vehicles* (Elsevier, Amsterdam, 2010).
- [9] S. Lübeck, M. Schreckenberg, and K. D. Usadel, *Phys. Rev. E* **57**, 1171 (1998).
- [10] K. Nagel, *Int. J. Mod. Phys. C* **5**, 567 (1994).
- [11] M. Gerwinski and J. Krug, *Phys. Rev. E* **60**, 188 (1999).
- [12] N. Bain, T. Emig, F.-J. Ulm, and M. Schreckenberg, *Phys. Rev. E* **93**, 022305 (2016).
- [13] A. Balouchi and D. A. Browne, *Phys. Rev. E* **93**, 052302 (2016).
- [14] A. M. C. Souza and L. C. Q. Vilar, *Phys. Rev. E* **80**, 021105 (2009).
- [15] M. Schreckenberg, A. Schadschneider, K. Nagel, and N. Ito, *Phys. Rev. E* **51**, 2939 (1995).
- [16] R. Barlovic, A. Schadschneider, and M. Schreckenberg, *Physica A* **294**, 525 (2001).